RSC Advances

COMMUNICATION

View Article Online
View Journal | View Issue

Cite this: *RSC Adv.*, 2016, **6**, 48566

Received 14th March 2016
Accepted 1st May 2016

DOI: 10.1039/c6ra06689e

www.rsc.org/advances

Colorimetric detection of influenza A (H1N1) virus by a peptide-functionalized polydiacetylene (PEP-PDA) nanosensor†

Sinae Song,‡[a] Kab Ha,‡[a] Kyeonghye Guk,[ac] Seul-Gee Hwang,[ac] Jong Min Choi,[b] Taejoon Kang,[ac] Pankee Bae,[b] Juyeon Jung*[ac] and Eun-Kyung Lim*[a]

We developed a peptide-functionalized polydiacetylene (PEP-PDA) nanosensor for pandemic H1N1 virus (pH1N1) detection with the naked eye. A PDA nanosensor was fabricated by nano-precipitation and modified with PEP for the specific recognition of pH1N1. The PEP-PDA nanosensor showed unique chromatic properties involving a colour change from blue to red in the presence of pH1N1. We believe that this nanosensor can be applied for the development of a commercially available kit for pH1N1 detection.

Influenza viruses are a significant cause of morbidity and mortality worldwide. In 2009, influenza A virus was designated as a major threat to public health because of its high infectivity.[1–3] A rapid, sensitive detection method for influenza virus is required for the prevention and effective control of pandemics.[4–11]

There are several tests for virus detection, such as serological diagnosis, viral culture, molecular diagnosis, and so on. Antibodies are produced after the onset of influenza virus illness and can be detected using serological diagnostic techniques like hemagglutination inhibition assay (HIA), enzyme immunoassay (EIA), complement fixation and neutralization tests. More than 80% of reverse transcription polymerase chain reaction (RT-PCT) influenza virus has been found by using HIA or virus micro neutralization assay. However, the Center of Disease Control and Prevention (CDC) does not recommend this method for virus detection because it is not a convenient method as it requires two serum samples with accurate timing and also has long throughput.[12] Virus culture method as a major technique is adopted for influenza virus detection in many clinical settings, although this is time consuming. Molecular diagnostic tests are also commonly used to diagnose influenza virus because they can be performed rapidly, with high throughput and sensitivity. Traditional RT-PCR, RT-PCR with detection by enzyme-linked immunosorbent assay (ELISA), real-time RT-PCR, and nucleic acid sequence-based amplification (NASBA) are included in molecular diagnostic test.[13,14] PCR-based test are generally used due to their fast detecting ability, more sensitivity as well as specificity in comparison with viral culture. In 2008, CDC received US Food and Drug administration approval for a highly sensitive influenza PCR assay such as RT-PCR has recently replaced viral culture as the gold standard.[15] Since then, many modifications and highly sensitive methods based on PCR have been developed. However, in developing countries, it is not easy to use PCR techniques for primary health care setting because it needs trained personnel for sample preparation and additional analytical equipment. Therefore, they require rapid detection methods enabling clinical decision making close to patients, point-of-care (POC) diagnostics methods.[16] POC diagnostics plays a pivotal role in public health by reducing the time between diagnosis and treatment. Biosensors based on colorimetric assays are particularly suitable for POC diagnostics because they do not require specialized instrumentation or technical skills for use.[17] Colorimetric detection by the naked eye is widely accepted for its simplicity and practicality.[18,19] Among the many colorimetric detection approaches, polydiacetylene (PDA) has been extensively studied as a colorimetric sensing material, owing to its unique chromatic properties.[20–37] The self-assembly of diacetylene monomers into spherical PDA vesicles with a conjugated backbone of alternating double and triple bonds (ene–yene chain) occurs upon ultraviolet (UV) irradiation. Unperturbed PDA vesicles typically exhibit an intense blue color because of electronic absorption *via* a π–π*

[a]*Hazards Monitoring BioNano Research Center, Korea Research Institute of Bioscience and Biotechnology, 305-806, Daejeon, Republic of Korea. E-mail: eklim1112@kribb.re.kr; jjung@kribb.re.kr; Tel: +82-42-879-8456*

[b]*BioNano Health Guard Research Center, Korea Research Institute of Bioscience and Biotechnology (KRIBB), 305-806, Daejeon, Republic of Korea*

[c]*Major of Nanobiotechnology and Bioinformatics, School of Engineering, University of Science and Technology (UST), 217 Gajeong-ro, Yuseong-gu, Daejeon, 305-350, Republic of Korea*

† Electronic supplementary information (ESI) available: Experimental details; preparation and characterization of PCDA-NHS and PEP-PDA nanosensor, viruses and colorimetric detection of pH1N1 using PEP-PDA nanosensor. See DOI: 10.1039/c6ra06689e

‡ These authors contributed equally to this work.

transition of the electrons in the conjugated backbone. However, external stimuli such as temperature, pH and ligand–receptor interactions strain the conjugated backbone in PDA vesicles, increasing the energy gap and enabling the absorption of light of higher energy, thus resulting in a colorimetric change of the PDA vesicles from blue to red. Consequently, studies of PDA materials are expanding, particularly for biosensing applications.[24,25,27,29,31,37]

Here, we developed a peptide-functionalized polydiacetylene (PEP-PDA) nanosensor enabling detection of pandemic H1N1 virus (pH1N1) with the naked eye. As illustrated in Fig. 1, PDA nanoparticles were first formed by self-assembly of 10,12-pentacosadiynoic acid (PCDA) and its derivatives in the aqueous phase through nano-precipitation method, and this was followed by exposure to UV light to generate the blue-colored PDA nanosensor. For accurate recognition of pH1N1, the PDA nanosensor was modified with a peptide (PEP) enabling specific binding to the HA1 protein on pH1N1 to generate the PEP-PDA nanosensor. This peptide sequence was known to have a high affinity for the HA proteins of the H1 strain and already confirmed high affinity against H1N1 viruses compared with others (H3N2, H5N2, and H6N5).[1,19,38–43] With reference to its ability, we modified this peptide sequence with PDA nanosensors for colorimetric detection of influenza A (H1N1) virus. When PEP-PDA nanosensors contact with H1N1 viruses, the interaction of H1N1 viruses with PEP from PEP-PDA nanosensors generate enough steric repulsion at the PDA nanosensors surface which induce the perturbation of the conjugated ene–yne backbone of PDA, resulting in a colorimetric transition from blue to red.[19]

We synthesized PCDA-NHS to facilitate reaction with the peptide, and the NHS esters were coupled to the carboxyl groups of PCDA *via* an esterification process (Fig. S1 and ESI†).[33–35] The Fourier transform infrared (FTIR) spectra of PCDA and PCDA-NHS revealed methylene asymmetric and symmetric C–H stretching peaks at 2926 and 2854 cm^{-1}, respectively. However, the carboxylic acid stretching (–COOH) observed at 1698 cm^{-1} for PCDA was absent in PCDA-NHS, and a new peak centered at 1729 cm^{-1} was observed due to ester formation (–COO–) (Fig. S2†). A peak centered at 2.8 ppm corresponding to the NHS moiety was also observed; this peak was absent in PCDA (Fig. S3 and S4†). After confirmation of PCDA-NHS formation, PDA nanoparticles were formed using a mixture of PCDA and PCDA-NHS monomers (10 : 1 molar ratio) and photo-polymerization by UV irradiation at 256 nm. The formation of PDA nanosensors resulted in a color change of the solutions from colorless to blue (Fig. 2(a)). In addition, the nanosensors were slightly smaller because of monomer polymerization (PDA nanoparticles: 54.6 ± 0.7 nm and PDA nanosensor: 47.7 ± 2.2 nm). The PDA nanosensors exhibited absorption at 640 nm *via* a π-to-π* absorption within the linear π-conjugated polymer network, in contrast to the PDA nanoparticles (Fig. 2(b)).[44–47] As shown in Fig. 2(c), the shape of PDA nanosensors observed in dry conditions by TEM exhibited a spherical shape. During the drying process for TEM sample preparation, PDA nanosensors were mainly affected by van der Waals force between nanoparticles, so they could be present with the aggregated state.[48]

The conformation of PDA nanosensors was systematically perturbed by increasing temperature and pH (Fig. 3).[49–53] As the temperature increased, the dynamics of all segments within the PDA nanosensors increased, resulting in a shift in the absorption spectrum to a high-energy region and a change in the color transition from blue to red due to conformational change. As shown in Fig. 3(a), the color of the PDA nanosensors gradually changed from blue to red with increasing temperature, and a new absorption band at ~540 nm appeared in the absorption

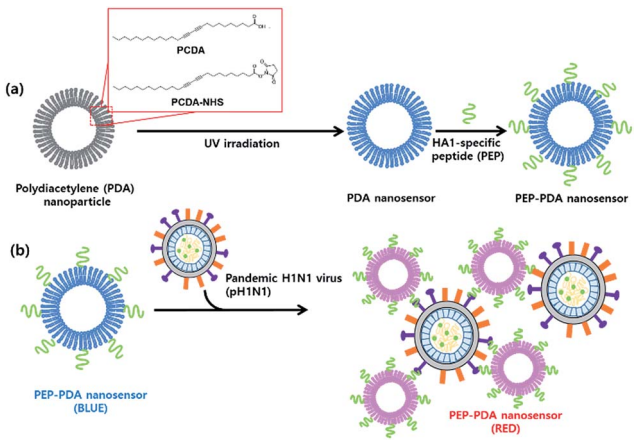

Fig. 1 Schematic illustration of the peptide-functionalized polydiacetylene (PEP-PDA) nanosensor for colorimetric detection of influenza A (pandemic H1N1) virus (pH1N1).

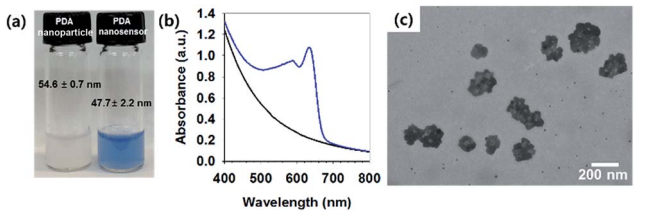

Fig. 2 (a) Color transition images of PDA nanoparticles and PDA nanosensors with size distribution (average ± standard deviation) and (b) absorption spectra (black: PDA nanoparticles and blue: PDA nanosensors). (c) TEM image of the PDA nanosensor after negative staining.

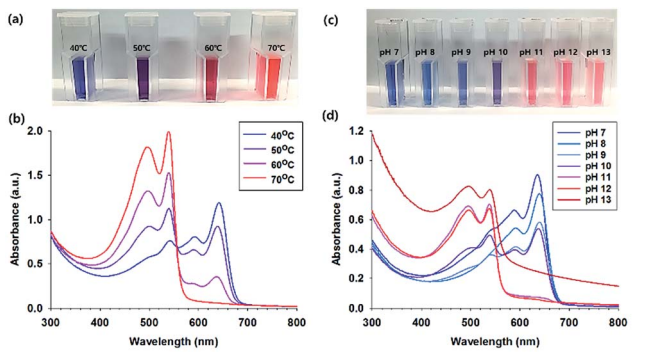

Fig. 3 Color transition images and absorption spectra of the PDA nanosensor after changes in temperature (a and b) and pH (c and d).

spectrum simultaneously with the disappearance of the absorption band at ~620 nm.[49,50] The dynamic of all PDA segments were promoted by increasing temperature. PDA segments could be rearranged by weakening inter- and intra-chain interactions within PDA nanosensors, which in turn altered the electronic state of conjugated backbone. Therefore, the HOMO–LUMON energy gap of perturbed PDA was widen upon increasing temperature, leading to the color transition from blue to red.[51–53] The PDA nanosensors also exhibited a color transition from blue to red with increasing pH (Fig. 3(b)). Under basic conditions, OH– ions abstracted the carboxylic protons of PCDA in the PDA nanosensors, leading to a systematic increase in the negatively charged carboxylate.[54,55] The segments of PDA nanosensors were rearranged, owing to the interruption of the dispersion interaction between the alkyl tails by the strong electrostatic repulsive force between their carboxylate groups (Fig. 3(c) and (d)).

Based on the unique chromic characteristics of the PDA nanosensors, we attempted to detect influenza A (H1N1) virus with the naked eye.[24,25,27,29,31,37] The PDA nanosensors were modified with a peptide (PEP) capable of specific binding with H1N1 virus, as confirmed in our previous report.[1] The colorimetric response of the PEP-PDA nanosensors in the presence of pH1N1 was confirmed by an obvious blue-to-red color change and a shift in the absorption spectrum. The magnitudes of these changes increased with the concentration of pH1N1 because higher pH1N1 concentrations-imposed higher stress on the PDA backbone. In contrast, the control PDA nanosensor modified by the control peptide did not exhibit any color change (Fig. 4). As shown in Fig. 4(b), in the absence of pH1N1, the PEP-PDA nanosensors displayed maximum absorbance at 628 nm and weaker absorbance at 550 nm, thus resulting in a blue color. The absorbance at 550 nm increased simultaneously with a decrease in the absorbance at 628 nm upon exposure to increasing concentrations of pH1N1, thus resulting in the observed color change from blue to red.

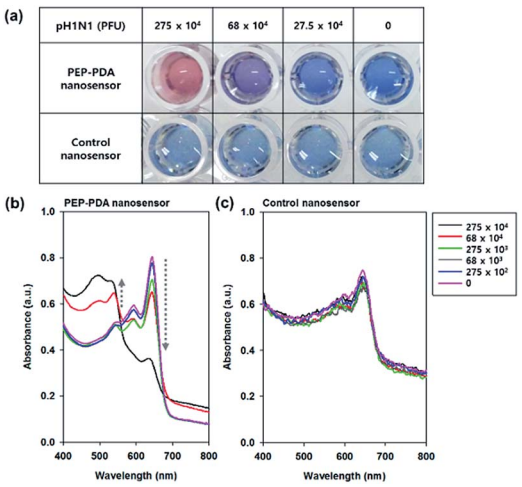

Fig. 4 (a) Color transition images after incubation of the PEP-PDA nanosensor and control nanosensor with different concentrations of pH1N1 and their absorption spectra ((b): PEP-PDA nanosensor and (c): control nanosensor).

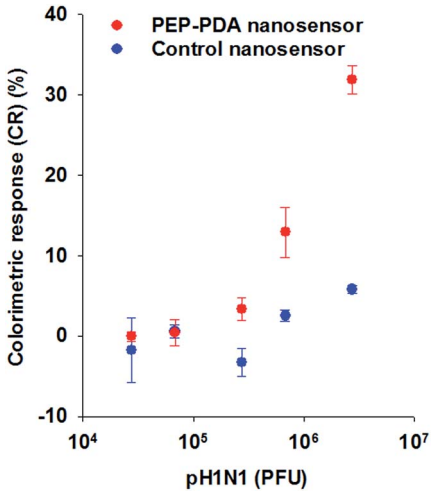

Fig. 5 Colorimetric response (CR) of the PEP-PDA nanosensor (red) and control nanosensor (blue) after incubation with varying concentrations of pH1N1. (CR (%) = $[(PB_0 - PB)/PB_0] \times 100$, where PB = $Abs_{628}/(Abs_{628} + Abs_{550})$). Error bars show the standard deviation of three experiments.

The color change depended on the amount of pH1N1 and was quantified by calculating the colorimetric response (CR). CR was determined from the change in the ratio of the absorbance (Abs) measurements at 550 nm (appears red) and 628 nm (appears blue) in the absence (PB_0) or presence (PB) of pH1N1 (CR (%) = $[(PB_0 - PB)/PB_0] \times 100$), where PB = $Abs_{628}/(Abs_{628} + Abs_{550})$.[12,26] Thus, a higher CR (%) value signifies a more efficient transition to the red color. As shown in Fig. 5, the CR (%) of the PEP-PDA nanosensor was approximately 32% and 13% at 2.75×10^6 PFU and 6.8×10^5 PFU of pH1N1, respectively. These results demonstrate that PEP-PDA nanosensor can be used to detect pH1N1 with the naked eye, with a detection limit of 10^5 PFU, *i.e.* about 0.2 HAU, indicating that it has sufficient sensitivity compared with conventional rapid diagnostic kits for influenza A virus.[56–58]

Conclusions

We fabricated a PEP-PDA nanosensor for pH1N1 detection with the naked eye that consists of PDA nanoparticles and a peptide enabling specific binding with the HA proteins of pH1N1. The PEP-PDA nanosensor was successfully used for specific detection of pH1N1 by an obvious blue-to-red color change. We expect that this nanosensor can be applied for the development of a commercially available kit for pH1N1 diagnosis.

Acknowledgements

The authors acknowledge financial support from the National Research Foundation of Korea (NRF) grant (NRF-2014M3A6B2060507 and H-GUARD_2014M3A6B2060489) funded by the Ministry of Education, Science and Technology

and by the KRIBB Research Initiative Program of the Republic of Korea.

Notes and references

1 E.-K. Lim, K. Guk, H. Kim, B.-H. Chung and J. Jung, *Chem. Commun.*, 2016, **52**, 175–178.
2 J. V. Kozlov, V. G. Gorbulev, A. G. Kurmanova, A. A. Bayev, A. A. Shilov and V. M. Zhdanov, *J. Gen. Virol.*, 1981, **56**, 437–440.
3 A. Manohar, *Braz. Arch. Biol. Technol.*, 2011, **54**, 15–23.
4 S. Y. Yi, U. Lee, B. H. Chung and J. Jung, *Chem. Commun.*, 2015, **51**, 8865–8867.
5 M. Igarashi, K. Ito, R. Yoshida, D. Tomabechi, H. Kida and A. Takada, *PLoS One*, 2010, **5**, e8553.
6 J. Vavricka, Y. Liu, H. Kiyota, N. Sriwilaijaroen, J. Qi, K. Tanaka, Y. Wu, Q. Li, Y. Li, J. Yan, Y. Suzuki and G. F. Gao, *Nat. Commun.*, 2013, **4**, 1491.
7 A. Ymeti, J. Greve, P. V. Lambeck, T. Wink, S. W. F. M. v. Hovell, T. A. M. Beumer, R. R. Wijn, R. G. Heideman, V. Subramaniam and J. S. Kanger, *Nano Lett.*, 2007, **7**, 394–397.
8 X. Zhang, A. N. Dhawane, J. Sweeney, Y. He, M. Vasireddi and S. S. Iyer, *Angew. Chem., Int. Ed.*, 2015, **54**, 5929–5932.
9 S. C. Gopinath, Y. Sakamaki, K. Kawasaki and P. K. Kumar, *J. Biochem.*, 2006, **139**, 837–846.
10 E. Noyola, B. Clark, F. T. O'donnell, R. L. Atmar, J. Greer and G. J. Demmler, *J. Clin. Microbiol.*, 2000, **38**, 1161–1165.
11 Y. Liu, L. Zhang, W. Wei, H. Zhao, Z. Zhou, Y. Zhang and S. Liu, *Analyst*, 2015, **140**, 3989–3995.
12 D.-K. Kim and B. Poudel, *Yonsei Med. J.*, 2013, **54**, 560–566.
13 D. L. Suarez, A. Das and E. Ellis, *Avian Dis.*, 2007, **51**, 201–208.
14 D. B. Jernigan, S. L. Lindstrom, J. R. Johnson, J. D. Miller, M. Hoelscher, R. Humes, R. Shively, L. Brammer, S. A. Burke, J. M. Villanueva, A. Balish, T. Uyeki, D. Mustaquim, A. Bishop, J. H. Handsfield, R. Astles, X. Xu, A. I. Klimov, N. J. Cox and M. W. Shaw, *Clin. Infect. Dis.*, 2011, **52**, S36–S43.
15 C. Chartrand, M. G. M. M. G. Leeflang, J. Minion, T. Bewer and M. Pai, *Ann. Intern. Med.*, 2012, **156**, 500–511.
16 W. D. Zhang and D. H. Evans, *J. Virol. Methods*, 1991, **33**, 165–189.
17 Y. K. Jung, T. W. Kim, H. G. Park and H. T. Soh, *Adv. Funct. Mater.*, 2010, **20**, 3092–3097.
18 Y. Liu, L. Zhang, W. Wei, H. Zhao, Z. Zhou, Y. Zhang and S. Liu, *Analyst*, 2015, **140**, 3989–3995.
19 A. Lesniewski, M. Los, M. Jonsson-Niedziólka, A. Krajewska, K. Szot, J. M. Los and J. Niedzolka-Jonsson, *Bioconjugate Chem.*, 2014, **25**, 644–648.
20 K. Lee, L. K. Povlich and J. Kim, *Analyst*, 2010, **135**, 2179–2189.
21 S. Qiu, Z. Lin, Y. Zhou, D. Wang, L. Yuan, Y. Wei, T. Dai, L. Luo and G. Chen, *Analyst*, 2015, **140**, 1149–1154.
22 C. H. Park, J. P. Kim, S. W. Lee, N. L. Jeon, P. J. Yoo and S. J. Sim, *Adv. Funct. Mater.*, 2009, **19**, 3703–3710.
23 D. A. Jose and B. König, *Chem. Commun.*, 2010, **8**, 655–662.
24 S. Seo, J. Lee, E.-J. Choi, E.-J. Kim, J.-Y. Song and J. Kim, *Macromol. Rapid Commun.*, 2013, **34**, 743–748.
25 Y. K. Jung, H. G. Park and J.-M. Kim, *Biosens. Bioelectron.*, 2006, **21**, 1536–1544.
26 O. Yarimaga, J. Jaworski, B. Yoon and J.-M. Kim, *Chem. Commun.*, 2012, **48**, 2469–2485.
27 D.-E. Wang, Y. Wang, C. Tian, L. Zhang, X. Han, Q. Tu, M. Yuan, S. Chen and J. Wang, *J. Mater. Chem. A*, 2015, **3**, 21690–21698.
28 M. A. Reppy and B. A. Pindzola, *Chem. Commun.*, 2007, **42**, 4317–4338.
29 H. Choi and J. S. Choi, *Bull. Korean Chem. Soc.*, 2013, **34**, 3083–3087.
30 X. Yan and X. An, *RSC Adv.*, 2014, **4**, 18604–18607.
31 Y. K. Jung, T. W. Kim, J.-M. Kim and H. G. Park, *Adv. Funct. Mater.*, 2008, **18**, 701–708.
32 N. Charoenthai, T. Pattanatornchai, S. Wacharasindhu, M. Sukwattanasinitt and R. Traiphol, *J. Colloid Interface Sci.*, 2011, **360**, 565–573.
33 J. Lee, M. Pyo, S.-h. Lee, J. Kim, M. Ra, W. Y. Kim, B. J. Park, C. W. Lee and J.-M. Kim, *Nat. Commun.*, 2014, **5**, 3736.
34 D.-H. Park, J. Hong, I. S. Park, C. W. Lee and J.-M. Kim, *Adv. Funct. Mater.*, 2014, **24**, 5186–5193.
35 S. Okada, S. Peng, W. Spevak and D. Charych, *Acc. Chem. Res.*, 1998, **31**, 229–239.
36 X. Yan and X. An, *Nanoscale*, 2013, **5**, 6280–6283.
37 Y. K. Jung, T. W. Kim, C. Jung, D.-Y. Cho and H. G. Park, *Small*, 2008, **4**, 1778–1784.
38 T. Matsubara, A. Onishi, T. Saito, A. Shimada, H. Inoue, T. Taki, K. Nagata, Y. Okahata and T. Sato, *J. Med. Chem.*, 2010, **53**, 4441–4449.
39 K. J. Oh, K. J. Cash, V. Hugenberg and K. W. Plaxco, *Bioconjugate Chem.*, 2007, **18**, 607–609.
40 S. Thurley, L. Roglin and O. Seitz, *J. Am. Chem. Soc.*, 2007, **129**, 12693–12695.
41 J. E. Kohn and K. W. Plaxco, *Proc. Natl. Acad. Sci. U. S. A.*, 2005, **102**, 10841–10845.
42 K. J. Oh, K. J. Cash, A. A. Lubin and K. W. Plaxco, *Chem. Commun.*, 2007, **6**, 4869–4871.
43 K. J. Oh, K. J. Cash and K. W. Plaxco, *Chemistry*, 2009, **15**, 2244–2251.
44 Y. B. Lee, J. M. Kim, K. H. Park, Y. G. Son, D. J. Ahn and J.-M. Kim, *Nanotech*, 2005, **2**, 434–437.
45 K. Sadagopan, S. N. Sawant, S. K. Kulshreshtha and G. K. Jarori, *Sens. Actuators, B*, 2006, **115**, 526–533.
46 J. Kim and J.-M. Kim, *Macromol. Res.*, 2006, **14**, 478–482.
47 N. Charoenthai, T. Pattanatornchai, S. Wacharasindhu, M. Sukwattanasinitt and R. Traiphol, *J. Colloid Interface Sci.*, 2011, **360**, 565–573.
48 E.-K. Lim, E. Jang, B. Kim, J. Choi, K. Lee, J.-S. Suh, Y.-M. Huh and S. Haam, *J. Mater. Chem.*, 2011, **21**, 12473–12478.
49 M. Gou, G. Guo, J. Zhang, K. Men, J. Song, F. Luo, X. Zhao, Z. Qian and Y. Wei, *Sens. Actuators, B*, 2010, **150**, 406–411.
50 C. P. Oliveira, F. Soares Nde, E. A. Fontes, T. V. Oliveira and A. M. Filho, *Food Chem.*, 2012, **135**, 1052–1056.

51 S. Toommee, R. Traiphol and N. Traiphol, *Colloids Surf., A*, 2015, **468**, 252–261.
52 A. Chanakul, N. Traiphol and R. Traiphol, *J. Colloid Interface Sci.*, 2013, **389**, 106–114.
53 A. Singh, R. B. Thompson and J. M. Schnur, *J. Am. Chem. Soc.*, 1986, **108**, 2785–2787.
54 A. Potisatityuenyong, R. Rojanathanes, G. Tumcharern and M. Sukwattanasinitt, *Langmuir*, 2008, **24**, 4461–4463.
55 A. Chanakul, N. Traiphol, K. Faisadcha and R. Traiphol, *J. Colloid Interface Sci.*, 2014, **418**, 43–51.
56 K. H. Chana, S. Y. Lama, P. Puthavathanab, T. D. Nguyenc, H. T. Longd, C. M. Panga, K. M. Chana, C. Y. Cheunga, W. H. Setoa and J. S. M. Peiris, *J. Clin. Virol.*, 2007, **38**, 169–171.
57 G. Boivin, S. Côté, P. Déry, G. Serres and M. G. Bergeron, *J. Clin. Microbiol.*, 2004, **42**, 45–51.
58 G.-C. Lee, E.-S. Jeon, W.-S. Kim, D. T. Le, J.-H. Yoo and C.-K. Chong, *Virol. J.*, 2010, **7**, 244–249.